Nanoscience and Nanotechnology Letters
Vol. 7, 162–165, 2015

An Efficient Design Method of Polymer Arrayed Waveguide Grating Multiplexer

Shuo Yang[1,2], Yong-Xin Sun[3], Bayanheshig[1], Yu-Hai Wang[3], and Zheng-Kun Qin[1,3,*]

[1] Changchun Institute of Optics Fine Mechanics and Physics, Chinese Academy of Sciences, Changchun 130033, China
[2] University of Chinese Academy of Sciences, Beijing 100049, China
[3] Jilin Normal University, Siping 136000, China

In this paper, a 17×17 arrayed waveguide grating (AWG) multiplexer with flat spectral response has been designed and fabricated by using FPE polymer materials. Experimental results show that the central wavelength is 1550.86 nm, and 3-dB bandwidth is about 0.478 nm, insertion loss is 10.5 dB, crosstalk is about −20.5 dB. Simulated results show that fabrication processing result in the shift of the transmission spectrum compared with the device theoretically designed. Furthermore, the transmission characteristics are discussed, and some efficient ways are reported.

Keywords: Arrayed Waveguide, Transmission Spectrum, Compensation, Crosstalk.

1. INTRODUCTION

The dense wavelength division multiplexing (DWDM) could provide an efficient way to enlarge the speed and capacity of current networks, the integrated optical wavelength multiplexer based on an arrayed waveguide grating (AWG) is a key device for DWDM system.[1–5] Recently, many research groups have fabricated some such optical devices using various polymeric materials.[6–12] However, simulated results show that fabrication process result in the shift of the transmission spectrum compared with the device theoretically designed. Therefore, it is very important how to analyze the fabrication process, and present some efficient ways.

Excellent AWG device is dependent on fine technology processing. However, manufacturing errors are hard to avoid in the fabrication of the AWG devices. It is hard to control the shape of the waveguide core in reactive ion etching process (RIE), and the core thickness in the process of spin-coating for polymer AWG advices. In this paper, based on the results of mass experiments, we can control the shape of the waveguide core and the core thickness through adjusting the experimental conditions, thus reduce the shift of the transmission spectrum. On the basis of the experiment results, it is suitable for the practical applications.

2. FABRICATION DETAILS

The guide core is buried in cladding, and the fabrication steps are shown in Figure 1 as follows:[12] (a) Spin-coating the under cladding and core layer in turn. In order to ensure the minimal stress-induced scattering, we spin and coat the under cladding two times, spin-coat at 1500 rmp, and increase its thickness to about 15 μm. We spin-coat the core layer at 3500 rmp, and its thickness is about 4 μm, and each curing of which is at 125 °C. (b) We deposit AI mask and increase its thickness to about 30 nm. (c) The BP-212 is chosen as Photolithographic material, spin-coat at 4000 rmp, curing of which is at 80 °C, and Photolithographic time is about 38s. (d) We dry-etch square waveguide patterns using RIE process, and select the optimized velocity of oxygen flow and etching power as 40 SCCM and 40 W, respectively. (e) We select the tetrahydrofuran (THF) as the solvent, and dissolving at 68 °C for 30 min. (f) The process of spin-coating the over cladding is same as which of spin-coating the under cladding. We have fabricated a polymer AWG advice through the above course. Figure 2 shows a scanning electron microscope (SEM) micrograph of the effect of the prepared the original design of the rectangular waveguide.

3. EQUIVALENT RECTANGULAR WAVEGUIDE

As can be seen from Figure 2, the cores of the channels and the arrayed waveguides exhibit smooth quasi-trapezoid cross-sections instead of originally designed rectangular ones. As pointed out above, the polymer AWG is usually formed by smooth quasi-trapezoid core cross-sections but originally designed rectangular ones after steam-dissolution. Based on the perturbation theory, we

*Author to whom correspondence should be addressed.

1941-4900/2015/7/162/004 doi:10.1166/nnl.2015.1895

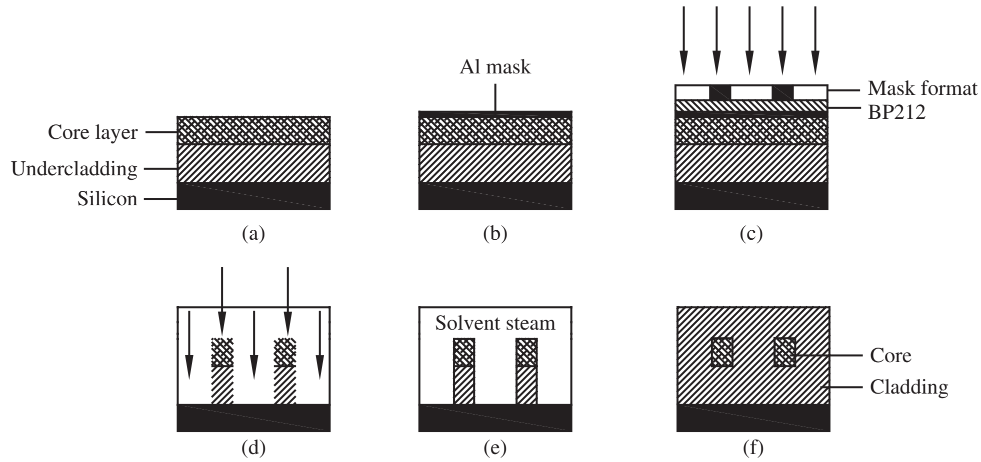

Fig. 1. Process steps of fabrication: (a) spin-coating the under cladding and core layer; (b) depositing metal mask, (c) photolithography, (d) RIE, (e)solvents steam; (f) spin-coating the over cladding.

present a technique named "equivalent rectangular waveguide method" to analyze the transmission characteristics of the AWG device with non-ideal core cross-sections. Figure 3 shows that we employ the "tanh" function to model this smooth quasi-trapezoid core cross-section, where, we can derive the expression of the $b(x)$ as follows Eq. (1).

$$b(x) = 0.5b\tanh\left(\frac{0.5a-|x|}{c}\right)/\tanh\left(\frac{0.5a}{c}\right) \quad (|x| \le a) \tag{1}$$

Where a and b are the core width and thickness of the originally designed rectangular waveguide respectively, and c is the shape factor of the "tanh" function. This can also be seen in the following Figure 1(b), that as the shape factor c decreases, the curve of the "tanh" function is close to a rectangle more and more. In the extreme case of $c = 0.2$ μm, the curve of the "$\tan h$" function plotted by the thick curve is close to the smooth quasi-trapezoid cross-section shown in Figure 3.

In order to meet the need of the design of AWG devices, we use an equivalent rectangular waveguide to replace the quasi-trapezoid waveguide, and let both the

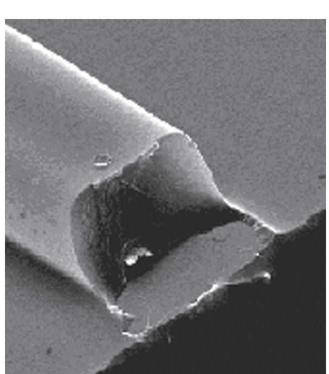

Fig. 2. SEM photograph of channel waveguide.

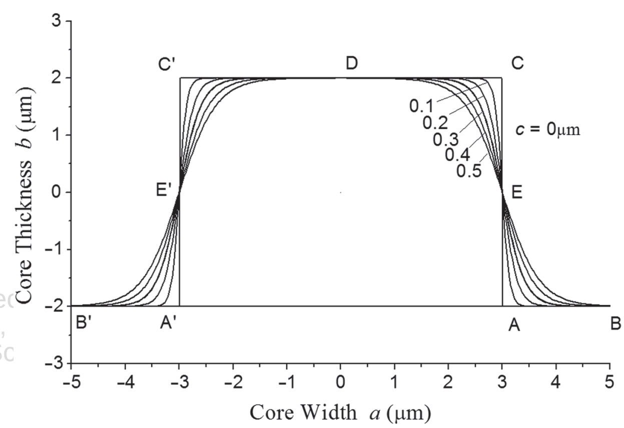

Fig. 3. Modeling curves of the core cross-section calculated from the "tanh" function.

propagation constants be equal to each other, where a_{eq} is the equivalent core width, which can be determined by the perturbation theory.[13] In this section, a_{eq} is 6 μm.

4. DESIGN OF AWG DEVICE

The FPE-51 is chosen as core material, and its refractive index is 1.5100. The styrene (St) is chosen as cladding material through regulating the mol percent of FPE-51 and FPE-49, and its refractive index is 1.4905. Based on these materials, we perform the parameter optimization of the polymer AWG multiplexer in Ref. [14]. The optimized values of the parameters are listed in Table I, and the AWG multiplexer is shown schematically in Figure 4.

5. FABRICATION ERROR ANALYSIS

Usually two kinds of main errors exist in the fabrication of polymer AWG devices, one is δa which is caused by the RIE process, and another is δb which results from the rotating-coating of the core thickness b. Because it is difficult to exactly control the experimental conductions, the

Table I. Optimum values of parameters of a polymer AWG with flat spectral response.

Central wavelength	$\lambda_0 = 1550.918$ nm
Wavelength spacing	$\Delta\lambda = 1.6$ nm
Width of guide core	$a = 6$ μm
Thickness of guide core	$b = 5$ μm
Width increment of guide core	$\delta a = 0.28$ μm
Pitch of adjacent waveguides	$d = 15$ μm
Refractive index of polymer guide core	$n_1 = 1.51$
Refractive index of polymer cladding	$n_2 = 1.4905$
Diffraction order	$m = 56$
Length difference of adjacent arrayed waveguides	$\Delta L = 57.8$ μm
Focal length of slab waveguide	$f = 7512$ μm
Free spectral range	FSR $= 13.77$ nm
Number of I/O channels	$2N+1 = 17$
Number of arrayed waveguides	$2M+1 = 99$

fabrication errors δa and δb would appear for the theoretically designed values of the core width a and the core thickness b. In addition, the cores of all the I/O channels and arrayed waveguides are formed by etching the same rotating-coating polymer film, therefore, they should nearly have the same width $a+\delta a$ and the same thickness $b+\delta b$, and hence the fabrication errors δa and δb should nearly have identical values for all the I/O channels and arrayed waveguides, respectively. So in the following calculations, we can assume that the fabrication errors δa and δb are constants, respectively.

We assume that the fabrication errors δa and δb change the core width from a to $a+\delta a$, and the core thickness from b to $b+\delta b$, and then δa and δb change the mode effective refractive index from n_c to $n_c+\delta n_c$. When the light with the central wavelength λ_0 passes through the AWG device from the central input channel to the central output channel, $\lambda = \lambda_0$, $\theta_{\text{in}} = \theta_{\text{out}} = 0$, then the grating equation is changed to $n_c \Delta L = m\lambda$. In this case, for the same diffraction order m, δn_c will make the central wavelength shift from λ_0 to $\lambda_0 + \delta\lambda$, then we can obtain the shift of the central wavelength $\delta\lambda$ as

$$\delta\lambda = \frac{\Delta L}{m}\left(\frac{\partial n_c}{\partial a}\delta a + \frac{\partial n_c}{\partial b}\delta b\right) \tag{2}$$

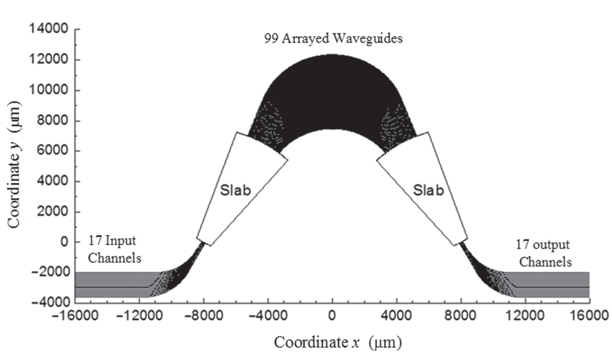

Fig. 4. Schematic layout of the designed polymer AWG device.

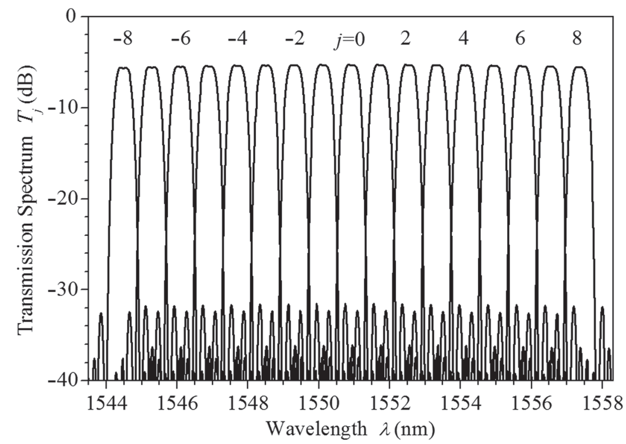

Fig. 5. Simulated transmission spectrum of the designed AWG.

where $\partial n_c/\partial a$ and $\partial n_c/\partial b$ can be determined by the eigenvalue equations of the E^y_{pq} mode of the rectangular waveguide.

When the δa and δb exist, which will change the mode effective refractive index from n_c to $n_c+\delta n_c$, in this case, using the diffraction theory of the AWG, we can derive the normalized distant field $E(\theta_{\text{out}})$ of all the 99 arrayed waveguides in the output slab as follows

$$\begin{aligned} E(\theta_{\text{out}}) = E_0(\theta_{\text{out}})\Bigg(1 + 2\sum_{v=1}^{M} E_0(v\Delta\theta) \\ \cdot\cos[vk(n_s d\sin\theta_{\text{in}} + n_c\Delta L + n_s d\sin\theta_{\text{out}} + \delta\phi)]\Bigg) \\ \cdot\left(1 + 2\sum_{v=1}^{M} E_0(v\Delta\theta)\right)^{-1} \end{aligned} \tag{3}$$

With

$$\begin{aligned} E_0(\theta) = k_x^2 q_x \cos\theta(q_x\cos(1/2k_s a\sin\theta) - k_s\sin\theta \\ \cdot\sin(1/2k_s a\sin\theta))\cdot((k_x^2 - k_s^2\sin^2\theta) \\ \cdot(q_x^2 + k_s^2\sin^2\theta))^{-1} \end{aligned} \tag{4}$$

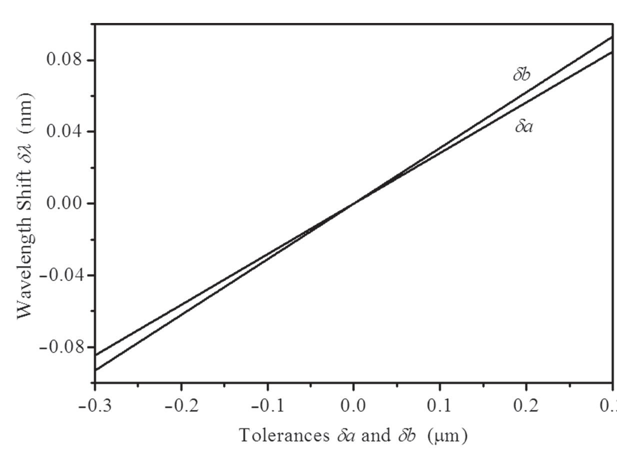

Fig. 6. The fabrication errors cause the wavelength shift.

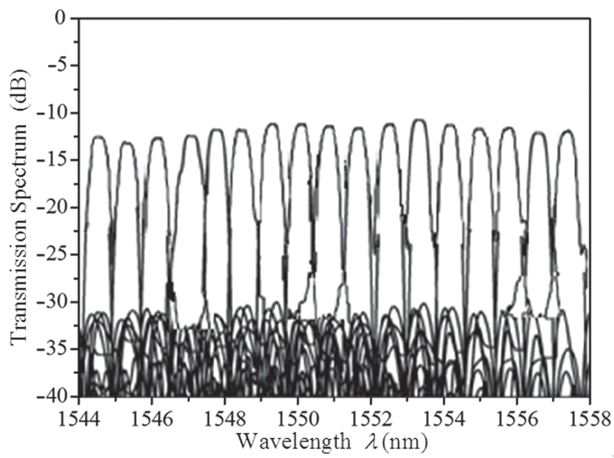

Fig. 7. Measured transmission spectrum of the fabricated AWG.

Where, $M = 49$, θ is the diffraction angle, $\Delta\theta = (mn_g\Delta\lambda)/(n_s n_c d)$ is the angle pitch of adjacent waveguides, $E_0(\theta)$ is the envelope function of $E_0(\theta_{\text{out}})$, $\Delta L_v = \Delta L_1 = \Delta L - \delta(\Delta L)$ for $v = 1, 3, 5, \ldots$, and $\Delta L_v = \Delta L_2 = \Delta L + \delta(\Delta L)$ for $v = 2, 4, 6, \ldots$ in Eq. (3), respectively. $\delta\phi = \Delta n_c \Delta L$ is the perturbation phase shift, which results from the fabrication errors δa and δb.

When the fabrication errors are not considered, that is $\delta a = \delta b = 0$, in this case, Figure 5 shows the transmission spectrum and the crosstalk of 17 output channels of the theoretically designed AWG device. When the fabrication errors are considered, that is $\delta a \neq 0$ or $\delta b \neq 0$, in this case, Figure 6 shows the effects of the fabrication errors δa and δb on the shift of transmission spectrum.

We find from Figure 6 that the fabrication errors cause the shift of the transmission spectrum. When the fabrication errors $\delta a, \delta b > 0$, the transmission spectrum shifts to the right. On the contrary, when $\delta a, \delta b < 0$, the transmission spectrum shifts to the left, compared with the theoretical design. When the values of the fabrication errors δa and δb are both positive or both negative, the accumulation of the fabrication errors would occur. When among the values of δa and δb, one is positive and another is negative, that is, $\delta a < 0$ and $\delta b > 0$, or $\delta a > 0$ and $\delta b > 0$, the compensation of fabrication errors would appear.

6. CONCLUSION

In order to guarantee the normal demultiplexing of the AWG device, fine manufacturing technology is required, and allowed fabrication errors need to be restricted strictly. On the basis of the preceding parameter optimization and manufacturing error analysis for a 17×17 polymer AWG multiplexer, an efficient compensation technique is reported for decreasing the spectral shift. By regulating the spin-coating rate and RIE conditions to control the polymer core thickness and the equivalent core widths, the spectral shift of the device can be reduced efficiently, a 17×17 AWG multiplexer with flat spectral response has been redesigned and fabricated. The measured transmission spectrum of the fabricated AWG in Figure 7, experimental results show that the central wavelength is 1550.86 nm, and 3-dB bandwidth is about 0.478 nm, insertion loss is 10.5 dB, crosstalk is about −20.5 dB.

Acknowledgment: The authors wish to express their gratitude to the National Science Foundation Council of China (11254001), and the Science and Technology Development of Jilin Province of China (20110320, 201201078) for their generous support to this work.

References and Notes

1. K. Maru, M. Okawa, Y. Abe, T. Hakuta, S. Himi, and H. Uetsuka, *Electron. Lett.* 43, 26 (**2007**).
2. Z. K. Qin and C. S. Ma, *Microwave and Optical Technology Letters* 52, 1653 (**2010**).
3. Y. K. Liu, S. C. Wang, Y. Y. Li, L. Y. Song, X. S. Xie, M. N. Feng, Z. M. Xiao, S. Z. Deng, J. Y. Zhou, J. T. Li, K. S. Wong, and T. F. Kraus, *Nature—Light: Science and Applications* 2, E52 (**2013**).
4. Z. K. Qin and C. S. Ma, *Microwave and Optical Technology Letters* 53, 273 (**2011**).
5. F. Song, J. Xiao, A. J. Xie, and S. W. Seo, *Journal of Optics* 16, 015503 (**2014**).
6. M. R. Amersfoort, C. R. de Boer, F. P. G. M. van Ham, M. K. Smit, P. Demeester, J. J. G. M. van der Tol, and A. Kuntze, *Electron. Lett.* 30, 300 (**1994**).
7. Y. P. Ho, H. Li, and Y. J. Chen, *IEEE Photon Technol. Lett.* 9, 342 (**1997**).
8. H. M. Zhang, C. S. Ma, Z. K. Qin, X. Z. Zhang, D. Zhang, S. Y. Liu, and D. M. Zhang, *Thin Solid Film* 515, 7313 (**2007**).
9. Z. K. Qin, H. P. Zhang, and G. F. Wang, *Optical Engineering* 52, 064601 (**2013**).
10. Y. Akihama and K. Hane, *Light: Science and Applications* 1, e16 (**2013**).
11. S. Jalilpiran, H. Karimi-Alavijeh, A. Katebi-Jahromi, and A. Gharavi, *Opt. Lett.* 36, 4125 (**2011**).
12. Z. K. Qin, Y. Yu, H. P. Zhang, G. F. Wang, Y. H. Wang, and C. S. Ma, *Microwave and Optical Technology Letters* 55, 2199 (**2013**).
13. D. L. Li, C. S. Ma, Z. K. Qin, Y. H. Wang, D. M. Zhang, and S. Y. Liu, *Journal of Optics A: Pure and Applied Optics* 9, 884 (**2007**).
14. C. S. Ma, Z. K. Qin, H. M. Zhang, H. Li, D. M. Zhang, and S. Y. Liu, *Microwave and Optical Technology Letters* 48, 916 (**2006**).

Received: 11 June 2014. Accepted: 14 July 2014.